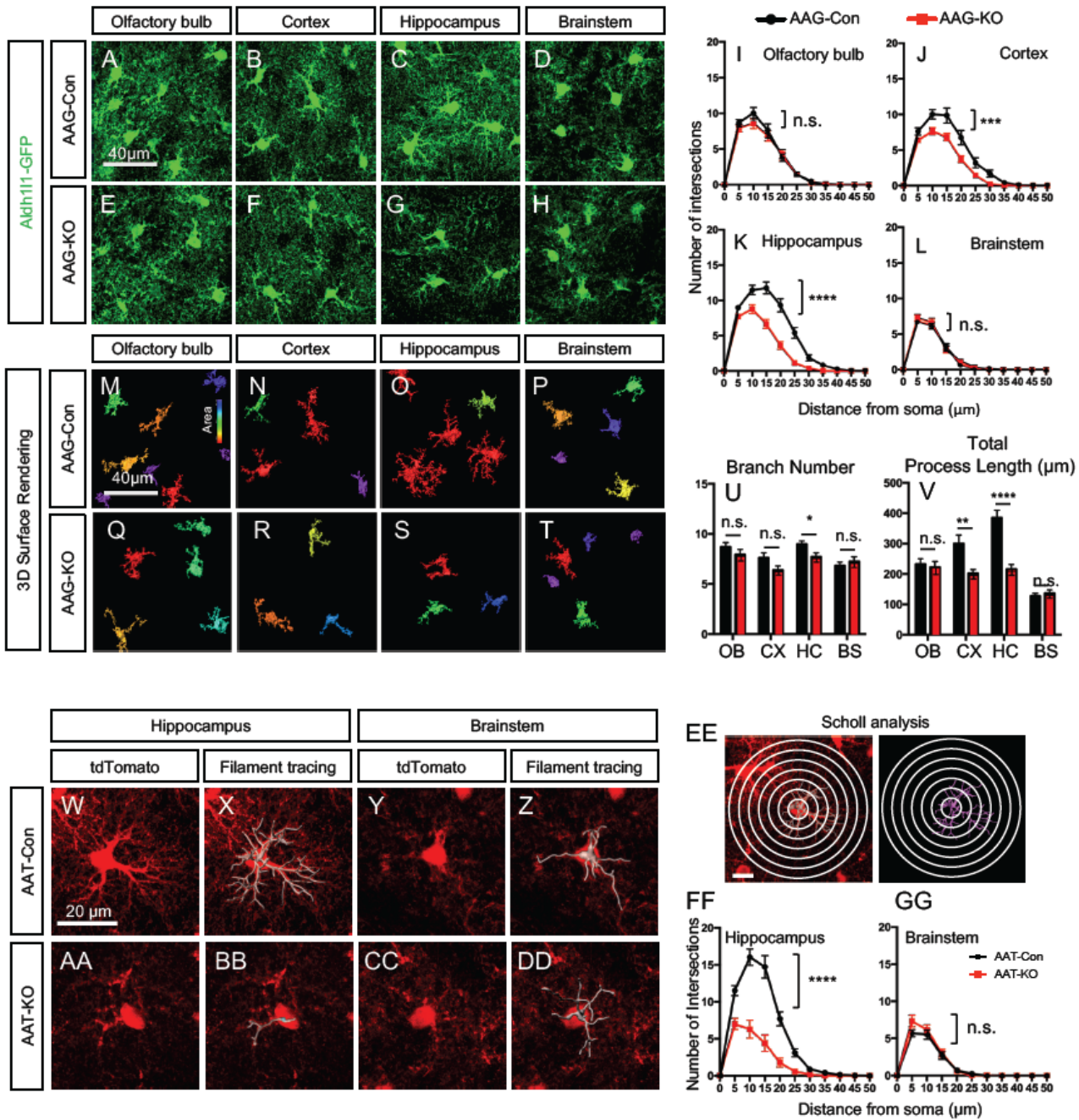
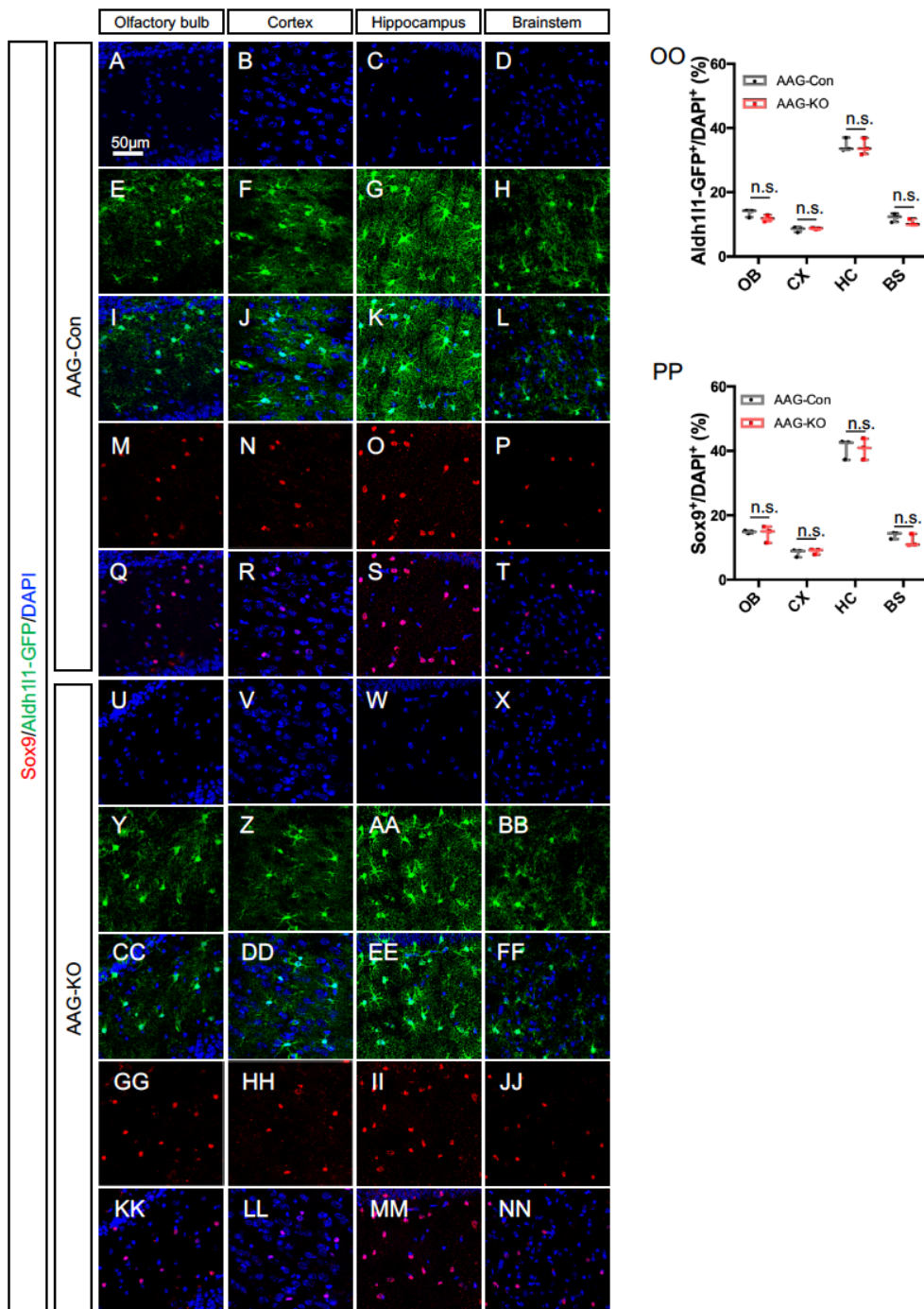


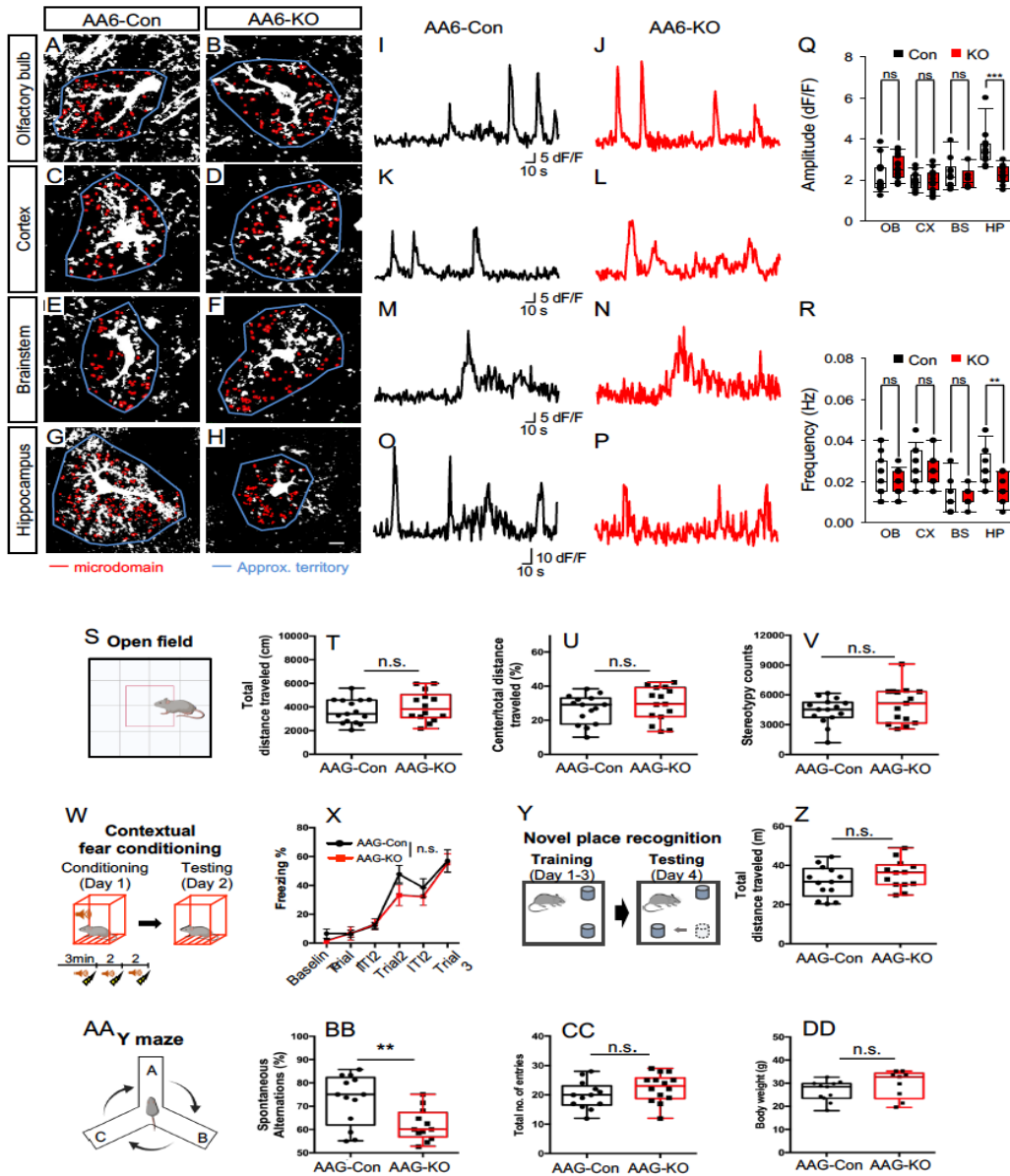
Supplemental Figure 1. Deletion of NFIA in mature astrocytes selectively alters astrocytes across diverse brain regions; Related to Figure 1. (A-H) Co-expression of NFIA and Aldh11-GFP from Aldh111-GFP mice. (I) Quantification of NFIA/Aldh11-GFP co-expression from Aldh11-GFP mice. Data derived from 4 mice, 3 slides with total of at least 100 cells per region, per mouse. Ordinary one-way ANOVA. (J-Y) Co-expression of NFIA and Aldh11-GFP from AAG-Con and AAG-KO mice as in Figure 1A-H, with single channel showing NFIA expression. (Z-GG) Expression of GFAP from AA-Con and AA-KO mice. (HH) Quantification of GFAP expression. OB: olfactory bulb; CX: cortex; HC: hippocampus; BS: brainstem. AAG-Con, denotes: *NFIA^{fl/fl}; Aldh11-GFP*. AAG-KO denotes: *NFIA^{fl/fl}; Aldh11-CreER; Aldh11-GFP*.



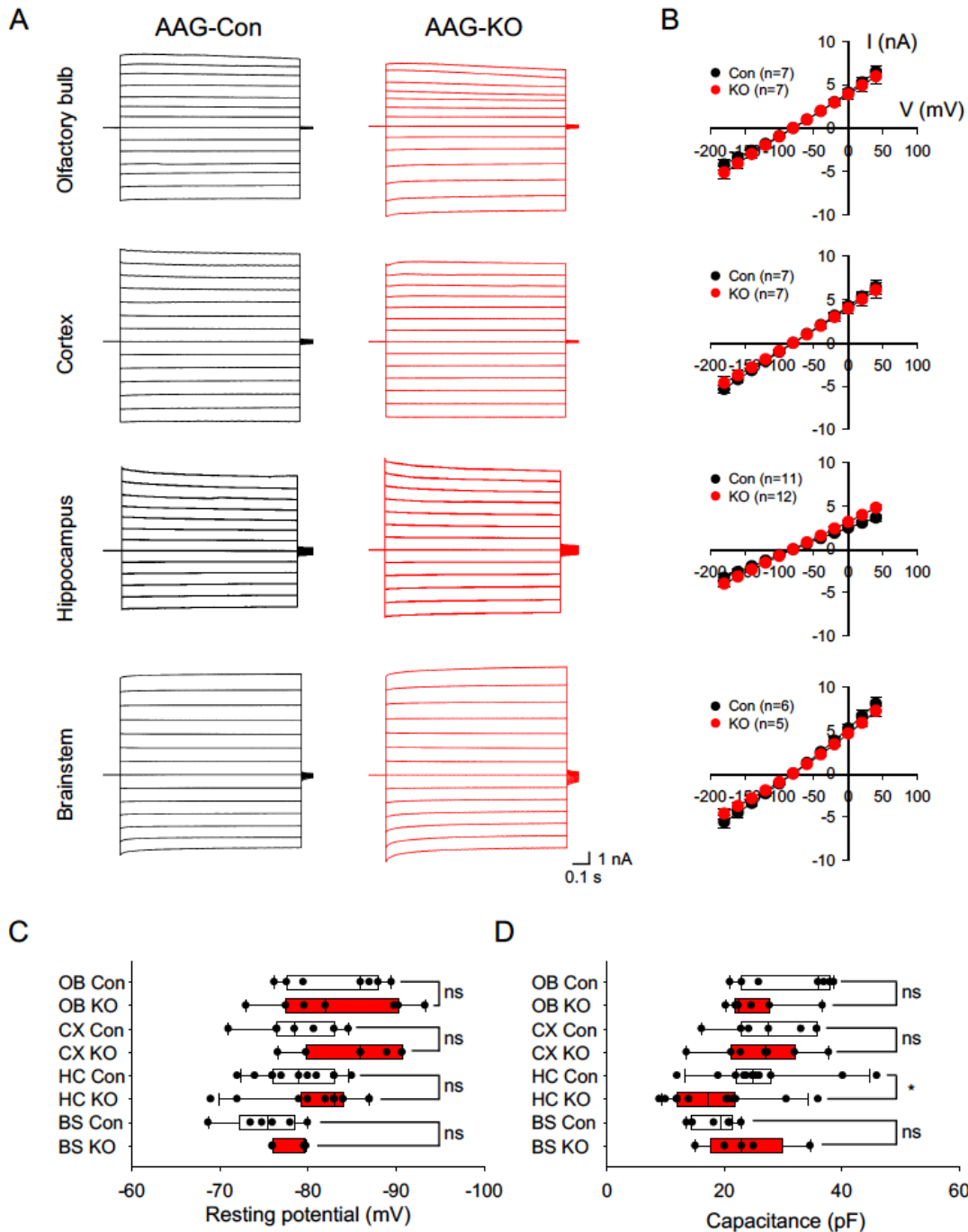
Supplemental Figure 2. Region-selective reduction of morphological complexity upon deletion of NFIA persists four months after NFIA deletion; Related to Figure 1. (A-H) Confocal images of Aldh111-GFP from AAG-con or AAG-KO mice. (I-L) Scholl Analysis of astrocyte complexity. Two-way repeated measures ANOVA. (M-T) 3D-surface rendering of confocal images from A-H. (U and V) Branch number and total process length quantification. Two-tailed unpaired t-test. In I-L and U-V, data is derived from 3 mice per genotype, 3 slides per region, per mouse, with at least 30 cells per region, per genotype. (W-DD) Confocal images and filament tracing from AAT-Con or AAT-KO mice in the hippocampus (W-BB) or the brainstem (Y-DD). (EE) example of Scholl analysis from AAT-con in the hippocampus. (FF, GG) Scholl analysis of astrocyte complexity. Two-way repeated measures ANOVA. OB: olfactory bulb; CX: cortex; HC: hippocampus; BS: brainstem. AAG-Con, denotes: *NFIA^{fl/fl}; Aldh111-GFP*. AAG-KO denotes: *NFIA^{fl/fl}; Aldh111-CreER; Aldh111-GFP*. AAT-Con denotes: *NFIA^{+/+}; Aldh111-CreER; Rosa-CAG-LSL-tdTomato*. AAT-KO denotes: *NFIA^{fl/fl}; Aldh111-CreER; Rosa-CAG-LSL-tdTomato*. * $p < 0.05$, ** $p < 0.01$, *** $p < 0.001$, and **** $p < 0.0001$.



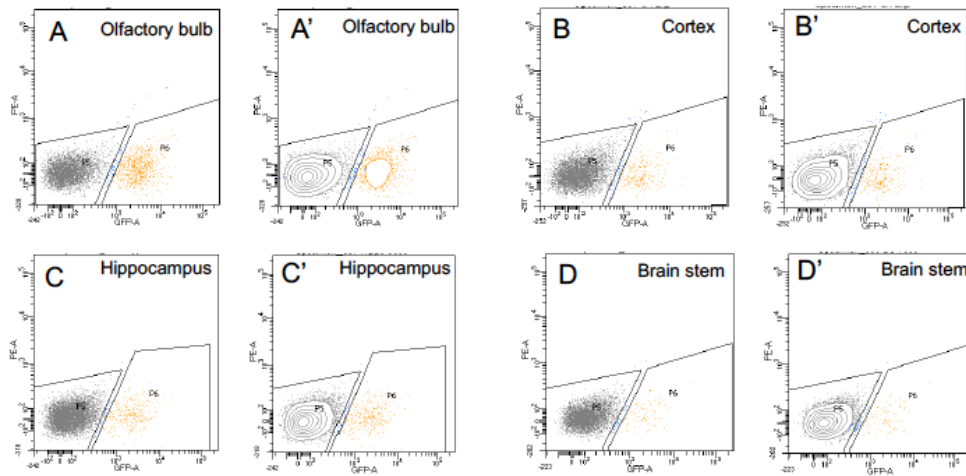
Supplemental Figure 3. Deletion of NFIA does not reduce the number of astrocytes across brain regions; Related to Figure 1. (A-D and U-X) Nuclear staining using 4',6-diamidino-2-phenylindole (DAPI) from AAG-con or AAG-KO mice. (E-H and Y-BB) Astrocyte labeling using Aldh111-GFP from AAG-con or AAG-KO mice. (I-L and CC-FF) Colabeling of Aldh111-GFP and DAPI showing % of astrocyte number (GFP+) among total cell number (DAPI+), as represented in (OO). (M-O and GG-JJ) Astrocyte labeling using Sox9 from AAG-con or AAG-KO mice. (Q-T and KK-NN) Colabeling of Sox9 and DAPI showing % of astrocyte number (Sox9+) among total cell number (DAPI+), as represented in (PP). (OO) Quantification of Aldh111-GFP/DAPI co-expression from AAG-con or AAG-KO mice. (PP) Quantification of Sox9/DAPI co-expression from AAG-con or AAG-KO mice. Data is derived from 3 mice per genotype, 3 slides per region, per mouse, with at least 500 cells per region, per animal, at 4 month post-induction. OB: olfactory bulb; CX: cortex; HC: hippocampus; BS: brainstem. AAG-Con, denotes: *NFIA^{fl/fl}; Aldh111-GFP*. AAG-KO denotes: *NFIA^{fl/fl}; Aldh111-CreER; Aldh111-GFP*. Two-tailed unpaired t-test



Supplemental Figure 4. Impaired microdomain calcium activity in hippocampal astrocytes in the absence of NFIA and behavioral assays in NFIA-cKO mouse; Related to Figure 2. (A-P) Representative images and traces from AA6-Con and AA6-KO mice showing spontaneous GCaMP6s activity in astrocytes from olfactory bulb, cortex, brainstem, and hippocampus. Red line denotes microdomain. (Q,R) Quantification of somatic $\Delta F/F$ GCaMP6s signal amplitude (Q) and frequency (R) derived from 3 mice from each genotype, 10-15 cells per sample. OB: olfactory bulb; CX: cortex; HC: hippocampus; BS: brainstem. AA6-Con denotes: *NFIA*^{+/+}; *Aldh111-CreER*; *Rosa-CAG-LSL-GCaMP6s*. AA6-KO denotes: *NFIA*^{fl/fl}; *Aldh111-CreER*; *Rosa-CAG-LSL-GCaMP6s*. ***p*<0.01, ****p*<0.001, Student's two-tailed unpaired t-test. (S-T) Schematics and quantification of open field test. Different parameters in open field test including total distance traveled (T), time spent in the center (U), stereotypic activity (V) are shown. (W-X) Schematics and quantification of fear learning during conditioning phase. Freezing % in response to 3 unconditioned stimulus (US)-conditioned stimulus (CS) pairs was shown; ITI, intertrial interval. (Y-Z) Schematics and total distance traveled in novel place recognition. (AA-BB) Schematics and quantification of y maze test. Percentages of spontaneous alternation (BB) and total number of entries into all three arms (CC) were shown. (DD) Body weights of mice of different genotypes. Data is derived from 10~15 age-matched male mice per genotype. (T-V, Z, BB-DD) Two-tailed unpaired t-test (f) Two-way ANOVA. AAG-Con denotes: *NFIA*^{fl/fl}; *Aldh111-GFP*. AAG-KO denotes: *NFIA*^{fl/fl}; *Aldh111-CreER*; *Aldh111-GFP*. ***p*<0.01.



Supplemental Figure 5. Electrophysiological properties in astrocytes are unaffected by loss of NFIA; Related to Figure 2. (A) Representative traces of passive conductance in CA1 astrocytes upon varying the injected voltage from AAG-Con and AAG-KO. (B) I-V curves associated with the traces. Two-way ANOVA with Sidak test. (c,d) Quantification of resting membrane potential (C) and capacitance (D) derived from 3 mice from each genotype, 5-12 cells per sample. OB: olfactory bulb; CX: cortex; HC: hippocampus; BS: brainstem. AAG-Con, denotes: *NFIA^{fl/fl}; Aldh111-GFP*. AAG-KO denotes: *NFIA^{fl/fl}; Aldh111-CreER; Aldh111-GFP*. * $p < 0.05$, Student's two-tailed unpaired t-test.



E

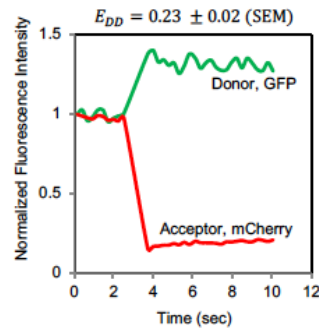
$$E_{DD} = 1 - \frac{I_{DA}}{I_D}$$

E_{DD} , FRET efficiency by donor dequenching

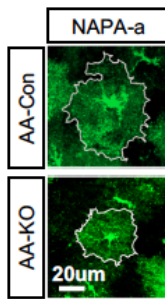
I_{DA} , donor intensity in the presence of acceptor

I_D , donor intensity after acceptor bleaching

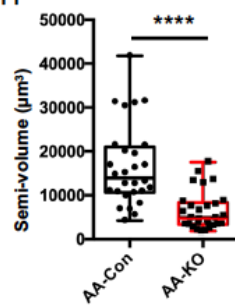
F



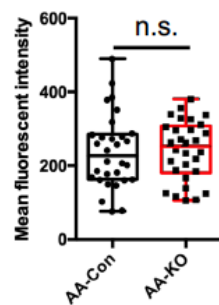
G



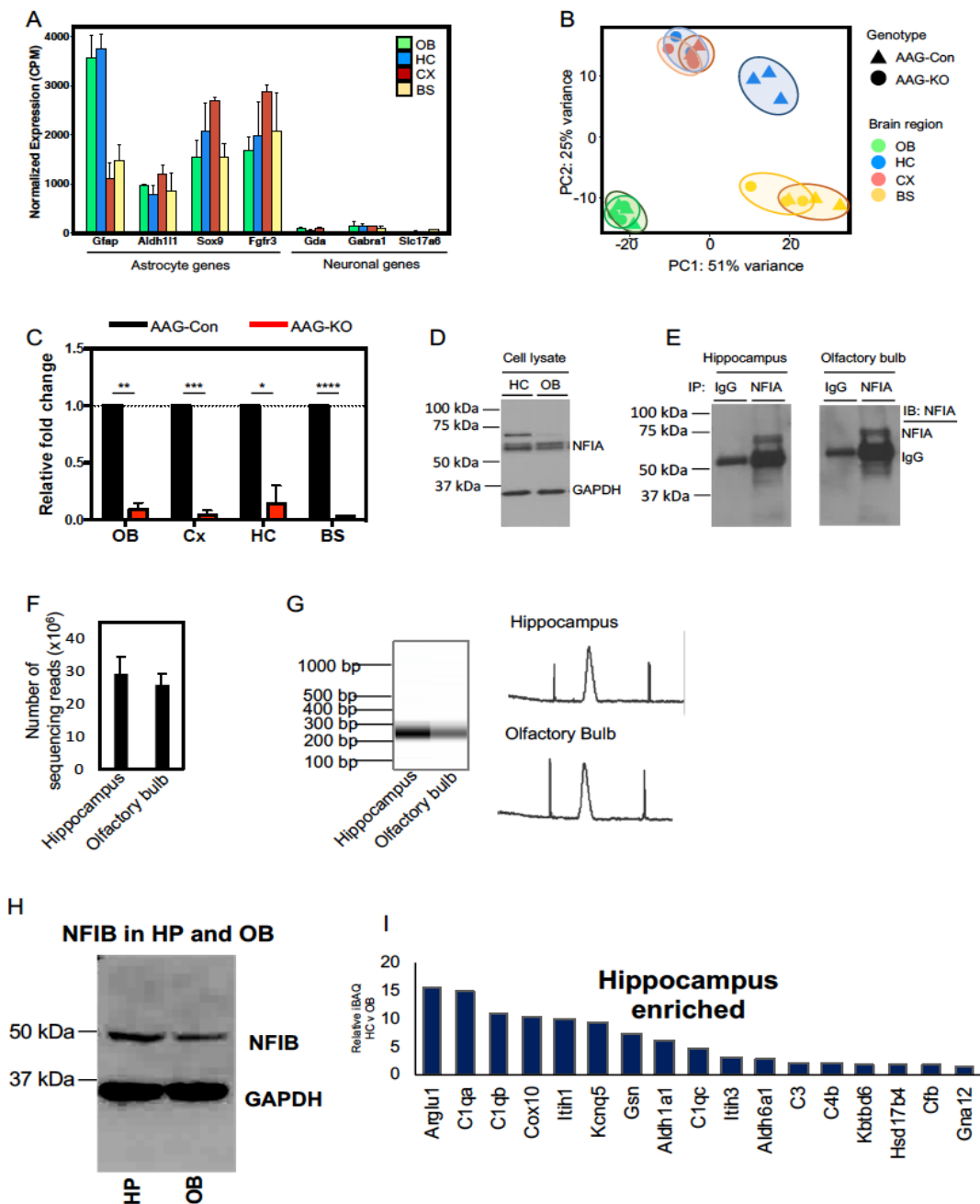
H



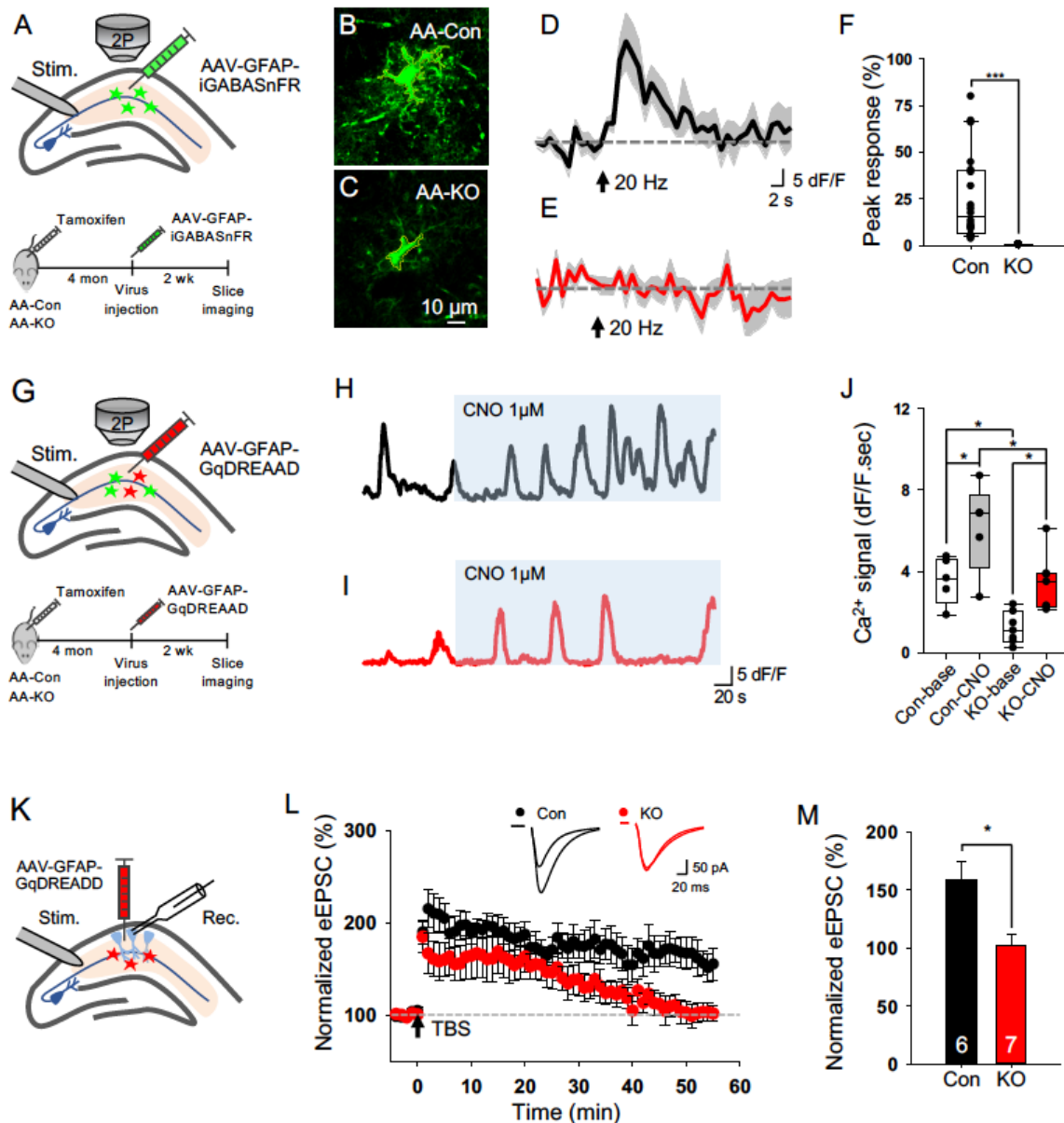
I



Supplemental Figure 6. Representative FACS plots from *Aldh111-GFP* mouse brains, donor dequenching measurement of FRET, and volume analysis; Related to Figures 3 and 5. *Aldh111-GFP* positive population was gated and GFP+ fraction was sorted in olfactory bulb (A and A'), cortex (B and B'), hippocampus (C and C'), and brainstem (D and D'). (A-D) and (A'-D') are different presentations of FACS plots. Data is derived from 3 mice per genotype at P160. (E) Equation for determining FRET efficiency in donor dequenching experiments. (F) Representative traces of donor (GFP) and acceptor (mCherry) fluorescence intensity upon photobleaching of acceptor. (G) Representative images of NAPA-a from AA-Con and AA-KO animals as in Figure 4d and 4h. (H) Volume analysis of astrocytes within 30 µm z-range (semi-volume) calculated by NAPA-a signal. (I) Mean fluorescent intensity of NAPA-a with individual astrocyte territory. Data is derived from 28~30 cells per genotype, 4 mice per genotype. AA-Con denotes: *NFIA^{fl/fl}*. AA-KO denotes: *NFIA^{fl/fl}; Aldh111-CreER*. Unpaired t-test. **** $p < 0.0001$.



Supplemental Figure 7. Quality controls for RNA-seq and ChIP-seq; Related to Figures 3 and 4. (A) Normalized relative expression of established astrocyte and neuronal genes across different brain regions. (B) Principal Component Analysis (PCA) of AAG-con or AAG-KO mice across brain regions. Note that loss of NFIA resulted in a shift of hippocampal astrocytes. (C) RT-qPCR validation of NFIA gene expression from AAG-con or AAG-KO mice across brain regions. (D) Western blot analysis of NFIA on protein extracts from the hippocampus or the olfactory bulb. (E) Western blot analysis from NFIA immunoprecipitation of cell lysates from hippocampus (HC) and olfactory bulb (OB) of 5-month old WT mice. IP, immunoprecipitation; IB, immunoblot. (F) Total number of sequencing reads from NFIA ChIP-Seq in the hippocampus and olfactory bulb, repeated 3 times (G) Representative Fragment Analyzer traces of NFIA ChIP-Seq DNA libraries from the hippocampus and olfactory bulb. (A-C) related to RNA-seq. (D-G) related to ChIP-seq. Data is derived from 3 mice per genotype at P160. (H) Immunoblot of NFIB from protein lysates taken from the olfactory bulb and the hippocampus. (I) NFIA-IP, mass spectrometry experiment showing list of proteins enriched in the hippocampus compared to the olfactory bulb.



Supplemental Figure 8. Impaired GABA sensing and LTP by loss of NFIA in astrocytes; Related to Figures 5 and 7. (A) Schematic of experimental workflow. (B-E) Representative images and traces from AA-con and AA-KO mice showing stimulation induced iGABASnFR activity in hippocampal CA1 astrocytes. (F) Quantification of peak response $\Delta F/F$ is derived from 3 mice from each genotype, 20 cells total. (G) Schematic of experimental workflow. (H,I) Representative CNO-induced Ca^{2+} activity from AAG-con and AAG-KO. (J) Quantification of area-under-curve (AUC) of Ca^{2+} signal. (K) Schematic of LTP experiment. (L) LTP traces from AAG-Con and AAG-KO hippocampal slices. (M) Quantification of LTP. *p < 0.05, ***p < 0.001, Student's two-tailed unpaired t-test (F,M), One-way ANOVA with Tukey's test (j). AA-Con denotes: *NFIA^{fl/fl}*. AA-KO denotes: *NFIA^{fl/fl}; Aldh111-CreER*. AAG-Con denotes: *NFIA^{fl/fl}; Aldh111-GFP*